Biarritz ARES 2 school
S4 : Clouds : condensation, haze & microphysics

Pierre Drossart

Institut d'Astrophysique de Paris

Plan

I. Condensation and clouds : thermodynamics of water clouds on Earth

II. Formation of hazes in planets and satellites :

- Jupiter
- Titan

III. The case of Jupiter Microphysics, thunderstorms

IV. Water clouds in exoplanets (K2-18b case)

Titan atmosphere compared to Earth

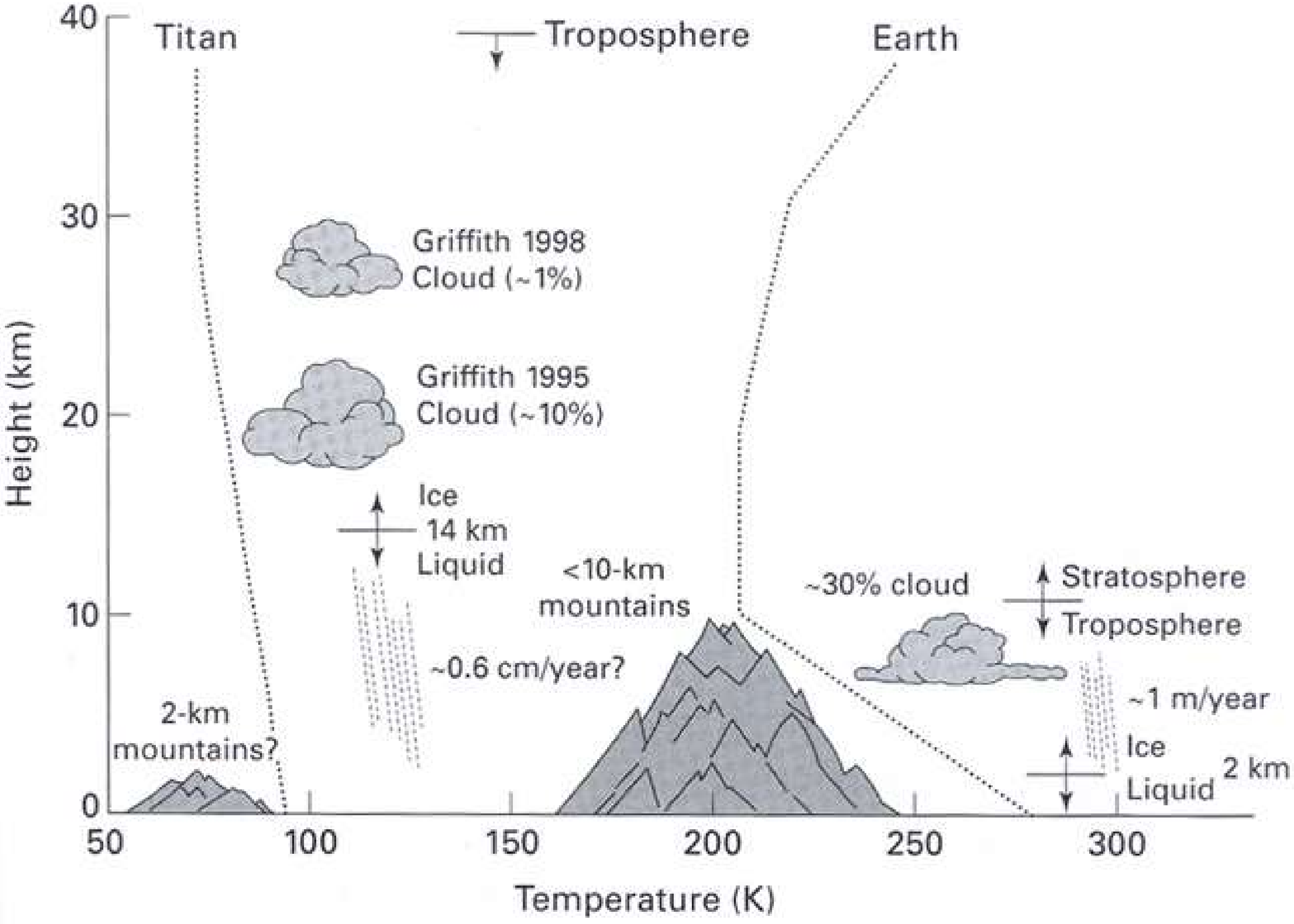

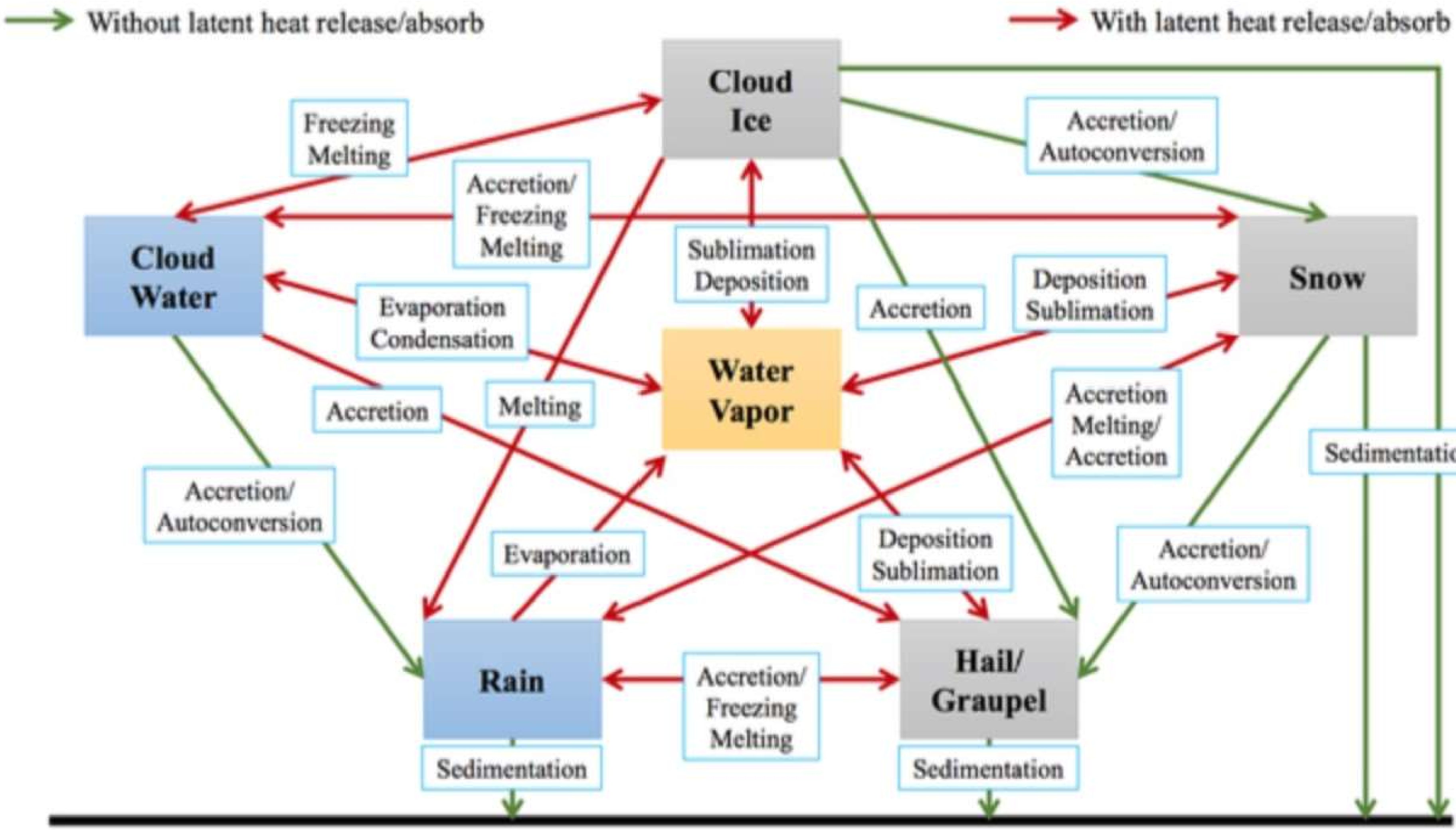
Without latent heat release/absorb
With latent heat release/absorb
Cloud Ice
Freezing
Melting
Accretion/
Autoconversion
Accretion/
Freezing
Melting
Cloud Water
Sublimation
Deposition
Snow
Deposition
Sublimation
Evaporation
Condensation
Accretion
Water Vapor
Accretion
Melting
Accretion
Melting/
Accretion
Sedimentation
Accretion/
Autoconversion
Evaporation
Deposition
Sublimation
Accretion/
Autoconversion
Rain
Accretion/
Freezing
Melting
Hail/
Graupel
Sedimentation
Sedimentation

Thermodynamics of the cloud formation

Ideally, if $P_i > P_{s,i}$ then condensation occurs removing i in the gas phase until $P_i = P_s$

The total condensate will be the $\int$ (Pi (z)– $Ps_{,i}$(T(z)))/(RT(z)) dz

Remarks:

- The base of the cloud is strictly defined as $P_i(z_0) = P_{s,i}(z_0)$
- The top of the cloud will depend on the total liquid content, and will vary with atmospheric vertical motions
- This equation if valid only in a quiescent non-convectively active atmosphere
- Due to the latent heat conversion in the condensation, a retroaction is present on the thermal profile : humid adiabatic gradient

Calculation of a humid adiabatic gradient

Thermodynamical equation :

Modified with respect to the dry equation $dH = VdP + Ldm_{vol}$

(for an adiabatic or isentropic displacement)

If $\Gamma = -g/C_p$ is the dry adiabatic gradient,

Then $\Gamma' = \Gamma / (1+L/C_p \, \partial e_{vol} / \partial T)$ where e_{vol} is the mass fraction of the volatile within the gas parcel.

	Vénus	Terre	Mars	Jupiter	Saturne	Uranus	Neptune	Titan
Γ (K/km)	-10.5	-9.8	-4.5	-2	-0.71	-0.67	-0.85	-1.3
Γ'(K/km)		-5						-0.5

Altitude of condensation

Knowing thermal profile + abundance of constituent

⇒Condensation level fully constrained in altitude (cloud base is a well – identified layer)

⇒Cloud depth : depends on the mass of condensable, on the convective activity, etc. => dynamical processes are important

=> Cloud deck not well constrained (reason why clouds seen from above are so sheepish…)

Formation of lenticular clouds

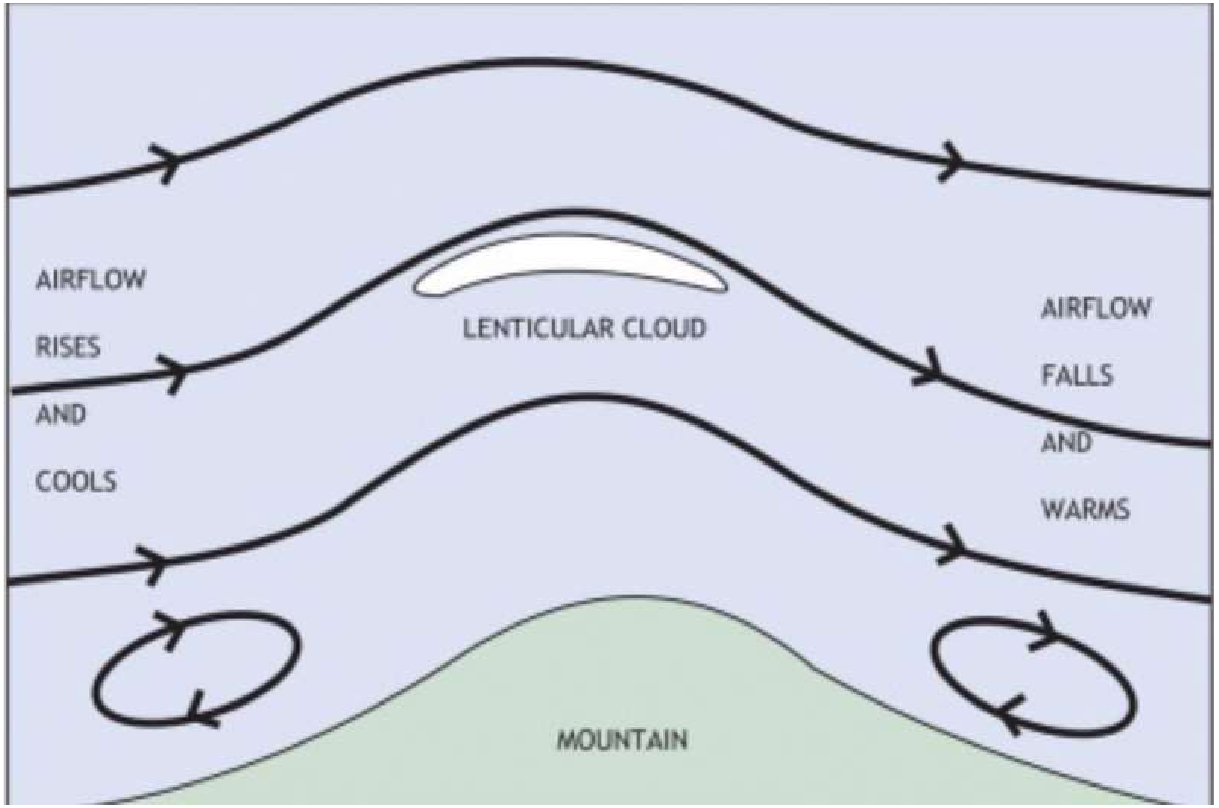

Lenticular clouds

Video
https://youtu.be/C_aNKioFDkg

Another interpretation is sometimes proposed…

Measurement of cloud altitudes by remote sensing

The problem of remote sensing :

We measure the cloud top, but the cloud bottom is more relevant for the thermodynamics of the atmopshere !

Extrapolating from top to bottom of clouds needs the knowledge of the volatile content in the cloud, a parameter which may depend on a lot of physical parameters (thermodynamics of condensation, dynamics, thermal structure)

Altimetry of the clouds top (day side)

Bands used for the altitude retrieval

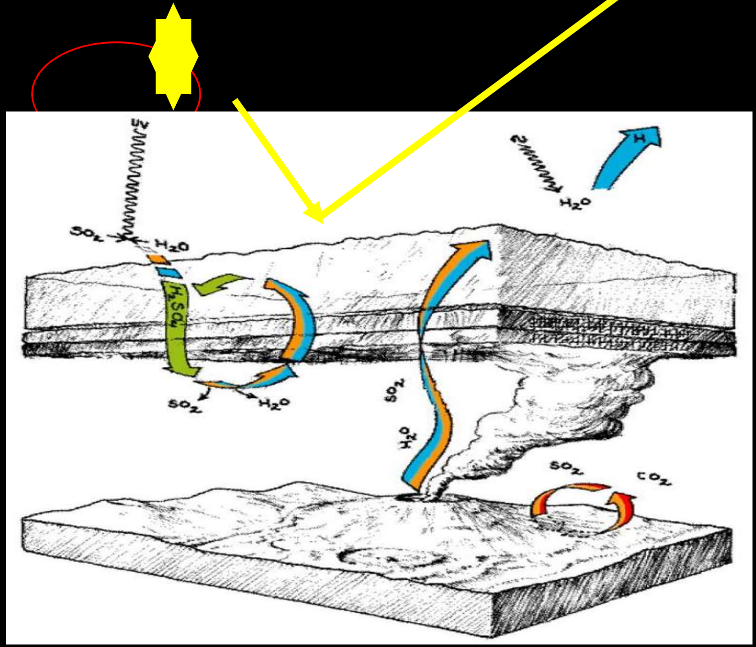

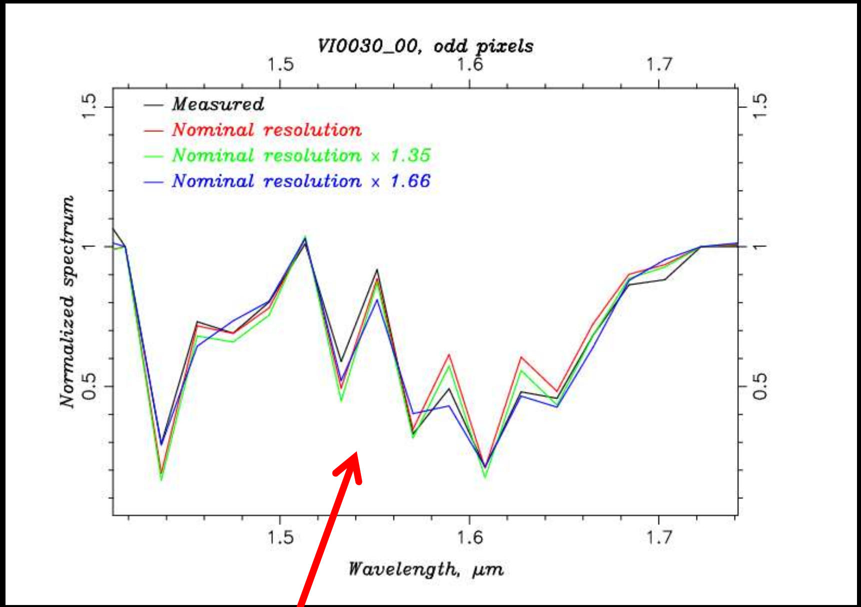

Altimetry

Cloud altitude measurements on Venus

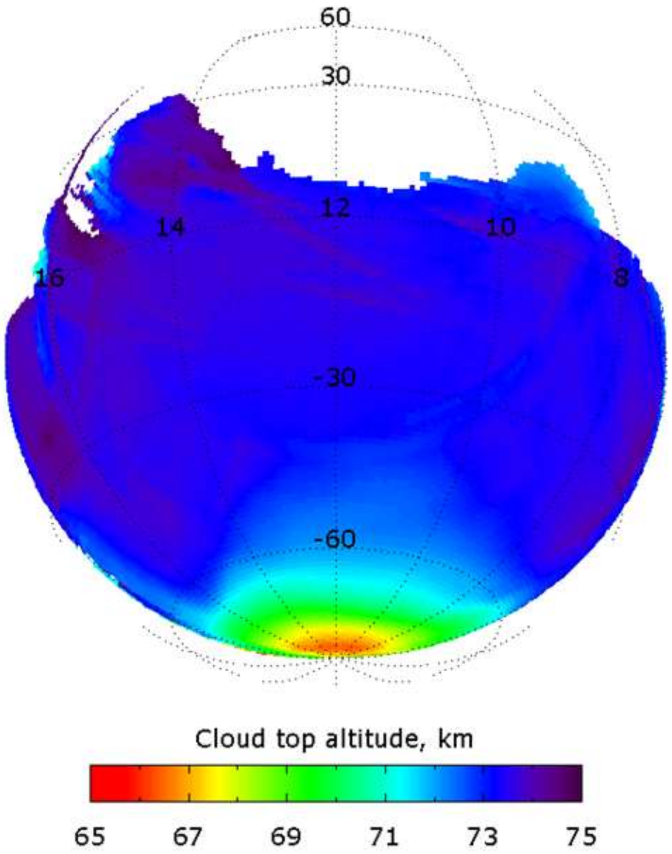

Measurement of the altitude of the upper cloud of Venus from CO_2 absorption

Atmospheric structure with clouds

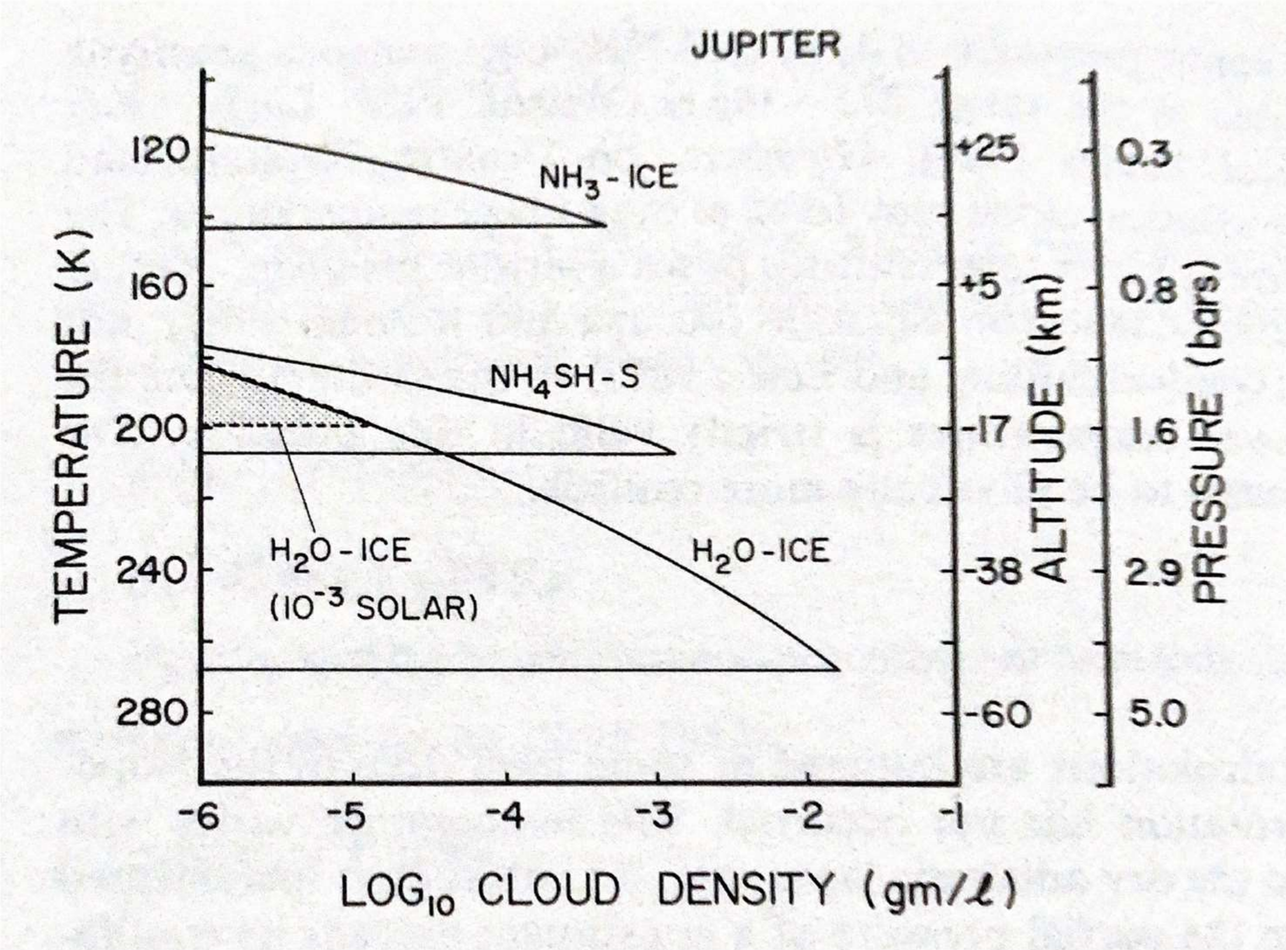

Introduction to polarization measurement : The Mie scattering

Maxwell equations for E, B field with boundary conditions on the surface of a sphere with refraction coefficients n_r , n_i

- Formulae

$$\begin{pmatrix} E_l^s \\ E_r^s \end{pmatrix} = \frac{\exp(-\mathrm{i}kr+\mathrm{i}kz)}{\mathrm{i}kr} \begin{pmatrix} S_2 & S_3 \\ S_4 & S_1 \end{pmatrix} \begin{pmatrix} E_l^i \\ E_r^i \end{pmatrix}$$

$$S_1(\theta) = \sum_{n=1}^{\infty} \frac{2n+1}{n(n+1)} \{a_n \pi_n(\cos\theta) + b_n \pi_n(\cos\theta)\}$$

$$S_2(\theta) = \sum_{n=1}^{\infty} \frac{2n+1}{n(n+1)} \{a_n \tau_n(\cos\theta) + b_n \pi_n(\cos\theta)\}$$

- properties

$$\pi_n(\cos\theta) = \frac{\mathrm{P}_n^1(\cos\theta)}{\sin\theta}, \qquad \tau_n(\cos\theta) = \frac{\mathrm{d}}{\mathrm{d}\theta}\mathrm{P}_n^1(\cos\theta),$$

Article : Hansen & Hovenier Venus, 1974

Interpretation of the Polarization of Venus

James E. Hansen

Goddard Institute for Space Studies, New York, N. Y. 10025

J. W. Hovenier

Dept. of Physics and Astronomy, Free University, Amsterdam, Netherlands

The linear polarization of sunlight reflected by Venus is analyzed by comparing observations with extensive multiple scattering computations. The analysis establishes that Venus is veiled by a cloud or haze layer of spherical particles. The refractive index of the particles is 1.44 ± 0.015 at $\lambda = 0.55$ μm with a normal dispersion, the refractive index decreasing from 1.46 ± 0.015 at $\lambda = 0.365$ μm to 1.43 ± 0.015 at $\lambda = 0.99$ μm. The cloud particles have a narrow size distribution with a mean radius of ~1 μm; specifically, the effective radius of the size distribution is 1.05 ± 0.10 μm and the effective variance is 0.07 ± 0.02. The particles exist at a high level in the atmosphere, with the optical thickness unity occurring where the pressure is about 50 mb.

The particle properties deduced from the polarization eliminate all but one of the cloud compositions which have been proposed for Venus. A concentrated solution of sulfuric acid (H_2SO_4-H_2O) provides good agreement with the polarization data.

Venus polarization

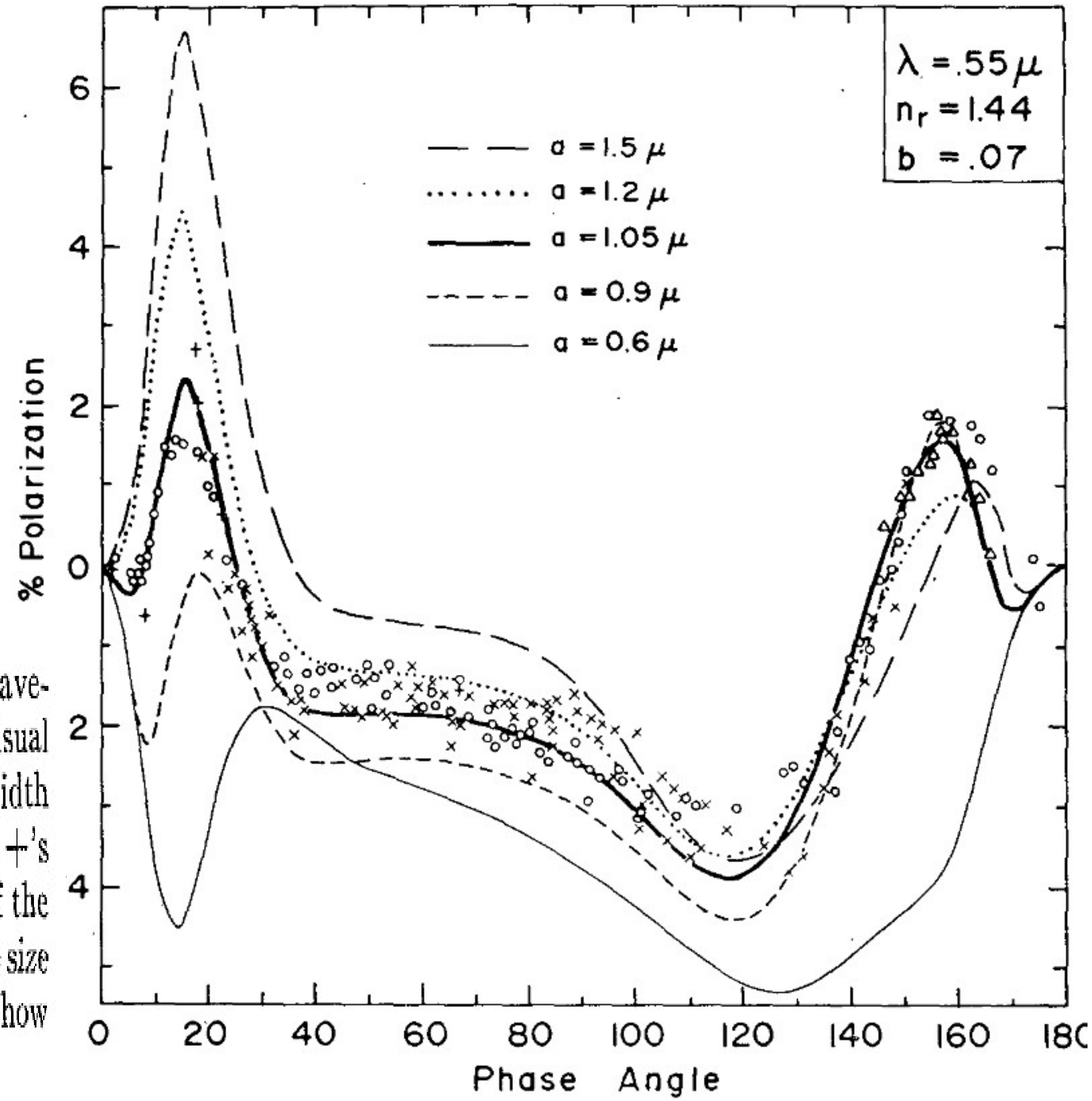

FIG. 4. Observations of the polarization of sunlight reflected by Venus in the visual wavelength region and theoretical computations for $\lambda=0.55$ μm. The O's are wide-band visual observations by Lyot (1929) while the other observations are for an intermediate bandwidth filter centered at $\lambda=0.55$ μm; the X's were obtained by Coffeen and Gehrels (1969), the +'s by Coffeen (cf. Dollfus and Coffeen, 1970), and the Δ's (which refer to the central part of the crescent) by Veverka (1971). The theoretical curves are all for a refractive index 1.44, the size distribution (8) with $b=0.07$, and a Rayleigh contribution $f_R=0.045$. The different curves show the influence of the effective radius on the polarization.

Retrieval of cloud scattering parameters

Refractive index : m=n-ir

Size distribution with r~1 µm and b=0.045

Atmospheric Rayleigh contribution

Compatible with H_2SO_4 cloud particles

1146 JOURNAL OF THE ATMOSPHERIC SCIENCES VOLUME 3

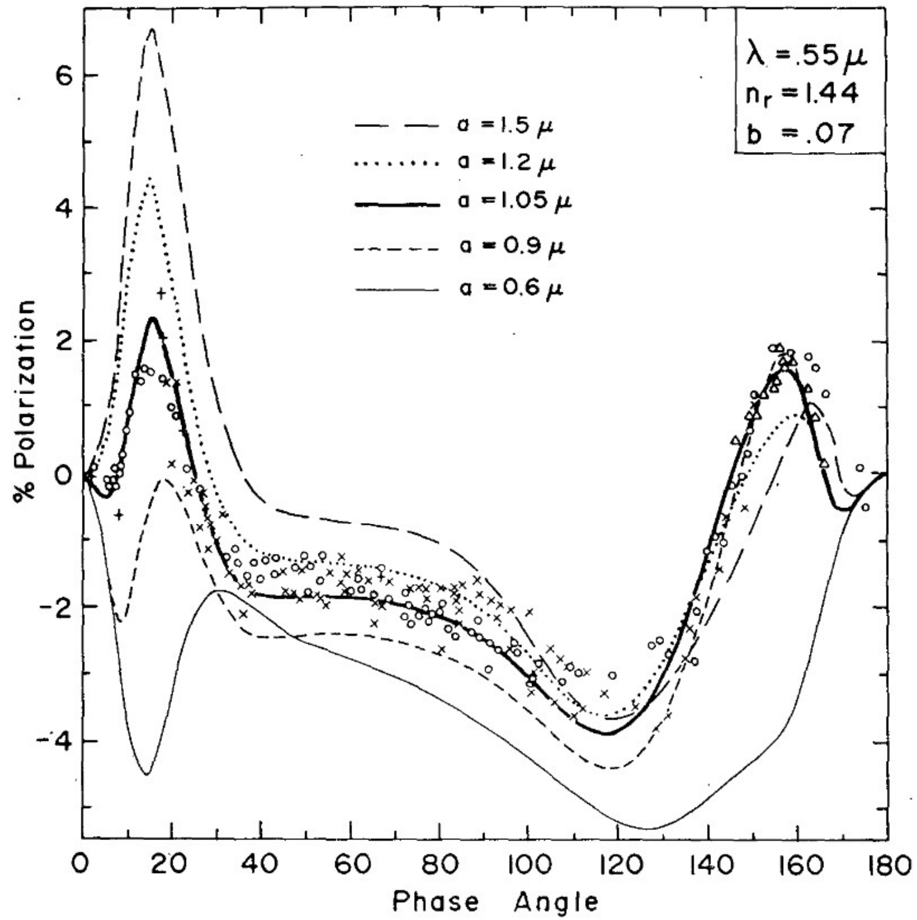

FIG. 4. Observations of the polarization of sunlight reflected by Venus in the visual wavelength region and theoretical computations for λ=0.55 µm. The ○'s are wide-band visual observations by Lyot (1929) while the other observations are for an intermediate bandwidth filter centered at λ=0.55 µm; the ×'s were obtained by Coffeen and Gehrels (1969), the +'s by Coffeen (cf. Dollfus and Coffeen, 1970), and the Δ's (which refer to the central part of the crescent) by Veverka (1971). The theoretical curves are all for a refractive index 1.44, the size distribution (8) with $b=0.07$, and a Rayleigh contribution $f_R=0.045$. The different curves show the influence of the effective radius on the polarization.

Jupiter clouds in polarized light

Cassini Huygens,

Wide angle camera with
CH4 filter + polarizer
Closest approach in 2000

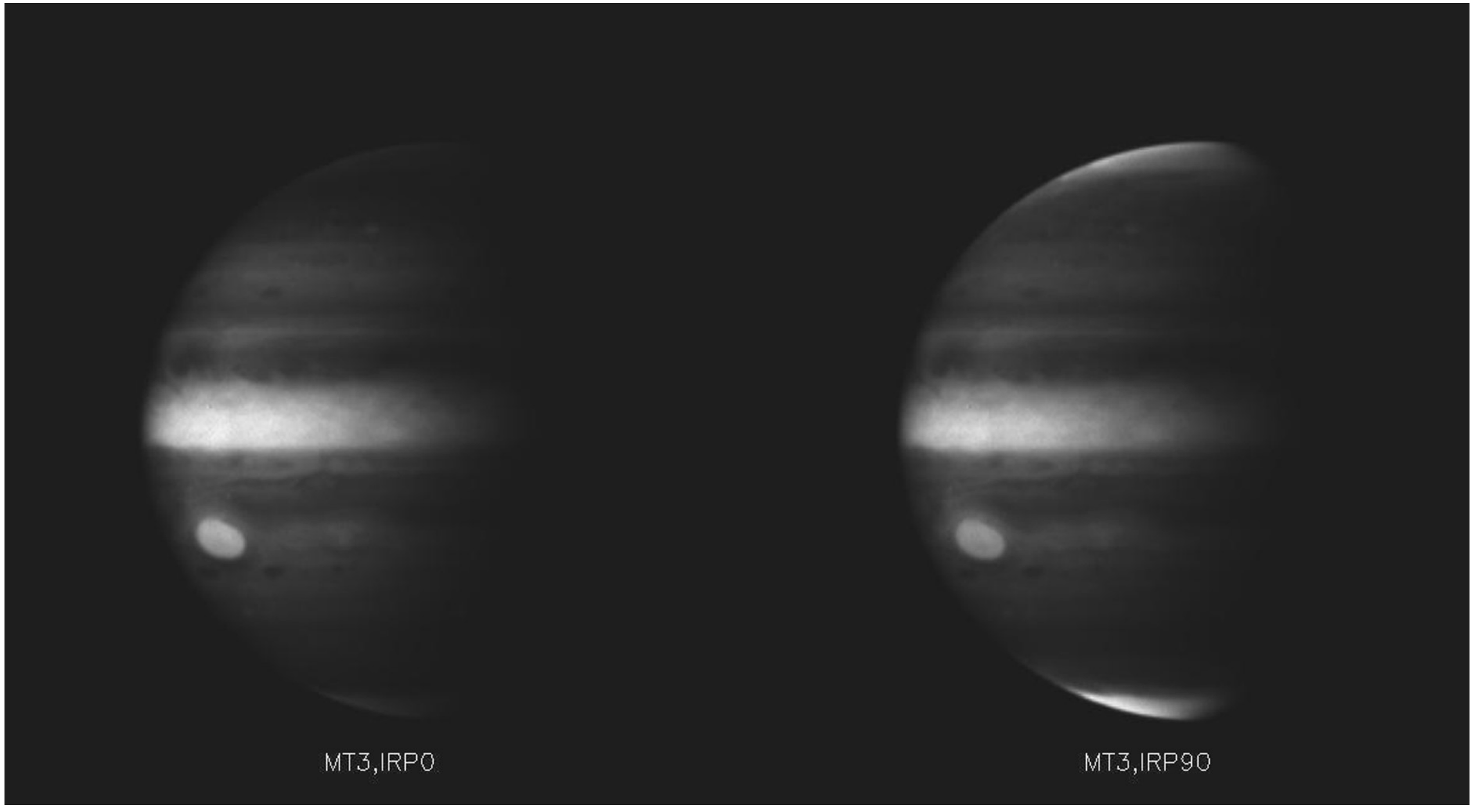

Poles appear bright in one image, and dark in the other. Polarized light is most readily scattered by aerosols. These images indicate that the aerosol particles at Jupiter's poles are small and likely consist of aggregates of even smaller particles, whereas the particles at the equator and covering the Great Red Spot are larger.

The formation of Titan’s haze

When sunlight or highly energetic particles from Saturn's magnetosphere hit the layers of Titan's atmosphere above about 600 miles (1,000 kilometers), the nitrogen and methane molecules there are broken up. This results in the formation of massive positive ions and electrons, which trigger a chain of chemical reactions that produce a variety of hydrocarbons. Many of these hydrocarbons have been detected in Titan's atmosphere, including polycyclic aromatic hydrocarbons (PAHs), which are large carbon-based molecules that form from the aggregation of smaller hydrocarbons. Some of the PAHs detected in the atmosphere of Titan also contain nitrogen atoms.

PAHs are the first step in a sequence of increasingly larger compounds. Models show how PAHs can coagulate and form large aggregates, which tend to sink, due to their greater weight, into the lower atmospheric layers. The higher densities in Titan's lower atmosphere favor the further growth of these large conglomerates of atoms and molecules. These reactions eventually lead to the production of carbon-based aerosols, large aggregates of atoms and molecules that are found in the lower layers of the haze that enshrouds Titan, well below about 300 miles (500 kilometers).

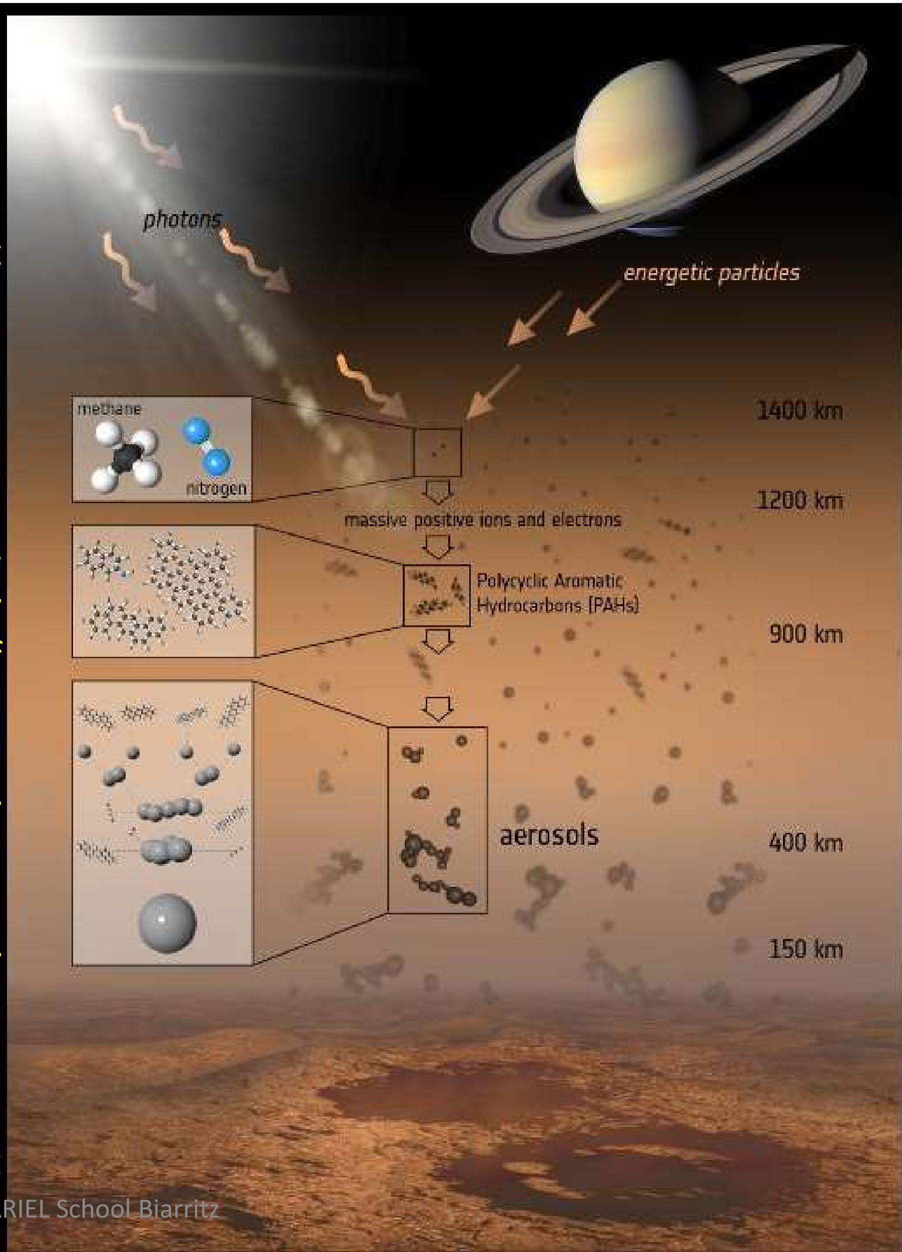

Credit : NASA/ESA

Three papers from Juno observations of Jupiter

Article | Published: 05 August 2020

Small lightning flashes from shallow electrical storms on Jupiter

Heidi N. Becker, James W. Alexander, Sushil K. Atreya, Scott J. Bolton, Martin J. Brennan, Shannon T. Brown, Alexandre Guillaume, Tristan Guillot, Andrew P. Ingersoll, Steven M. Levin, Jonathan I. Lunine, Yury S. Aglyamov & Paul G. Steffes

Nature **584**, 55–58(2020)

JGR Planets

Research Article | Free Access |

Storms and the Depletion of Ammonia in Jupiter: I. Microphysics of "Mushballs"

Tristan Guillot, David J. Stevenson, Sushil K. Atreya, Scott J. Bolton, Heidi N. Becker

First published: 05 August 2020 | https://doi.org/10.1029/2020JE006403 | Citations: 1

JGR Planets

Research Article | Free Access |

Storms and the Depletion of Ammonia in Jupiter: II. Explaining the Juno Observations

Tristan Guillot, Cheng Li, Scott J. Bolton, Shannon T. Brown, Andrew P. Ingersoll, Michael A. Janssen, Steven M. Levin, Jonathan I. Lunine, Glenn S. Orton, Paul G. Steffes, David J. Stevenson

First published: 03 August 2020 | https://doi.org/10.1029/2020JE006404 | Citations: 1

Lightning in Earth cumulonimbus

Not fully understood yet !

Most important ingredients :

- Light Ice crystals (up)
- Large supercooled droplets (down)
- Collisions make ice crystals (+) and droplets (–) charged
- Large convective structure => cycle of charge

=> Typical 10^6 V/m

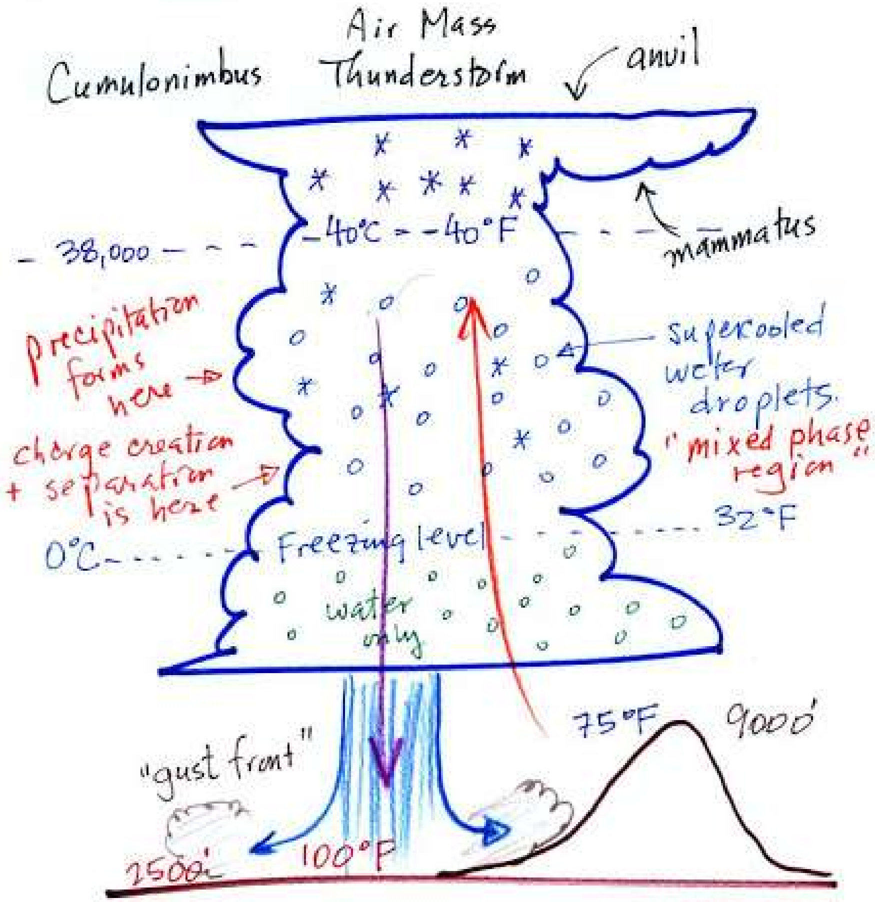

©University of Arizona, hydrology and atmospheric science dept

Cloud structure of Jupiter

Cloud structure of Jupiter for solar elemental ratios

⇒ predicts liquid water clouds and convective thunderstorms generation similar to Earth at p> 5 bar levels

⇒ According Voyager and Galileo observations, lightning occurs in the water liquid-ice clouds

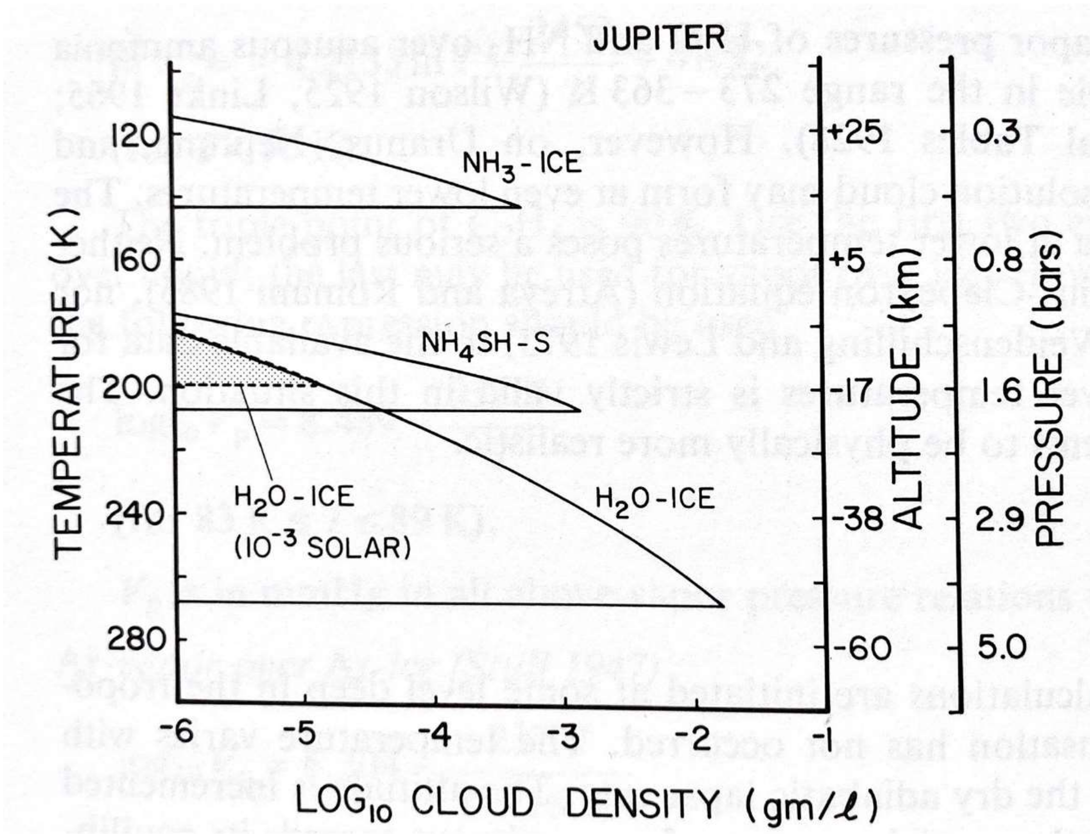

From S.K. Atreya, Atmospheres and Ionospheres of the Outer Planets and their Satellites, Springer-Verlag, 1986

New observations by JUNO : lightning on night side of Jupiter as observed by Juno SRU

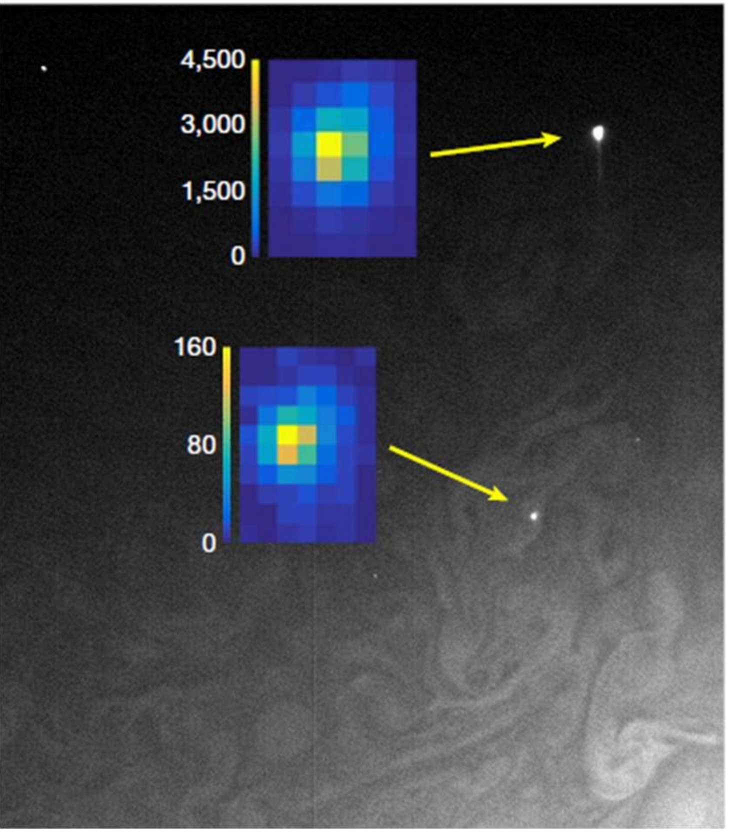

Images from Juno SRU Jovian lightning survey. Cloud top illumination from Io moonlight. Spread due to camera's PSF and incomplete motion compensation

Model of scattering within the cloud layers gives an estimate for an origin of flash around 1.4-1.9 bars

=> Question : what is the mechanism for ice particles-only lightning generation? Or is a new mechanism responsible ?

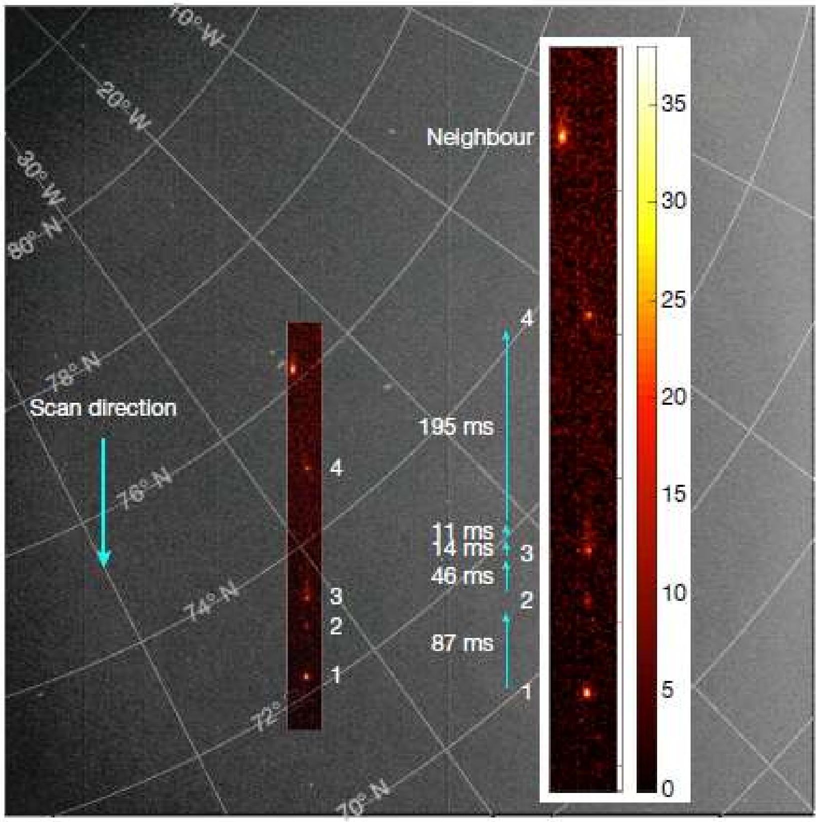

Becker et al, Nature, Fig. 1

Lightning generation on Jupiter

Illustration of lightning generation above and below the 3-bar level
Updraughts of water-ice particules up to 1.1-1.5 bar generates adsorption of NH_3 which melts the ice, creating liquid NH_3-H_2O particles

Charge separations is produces by collisions of NH_3-H_2O particles with water – ice. The limit for supecooled water is about 233 K (white line)

SRU lightning flashes characteristics are listed below

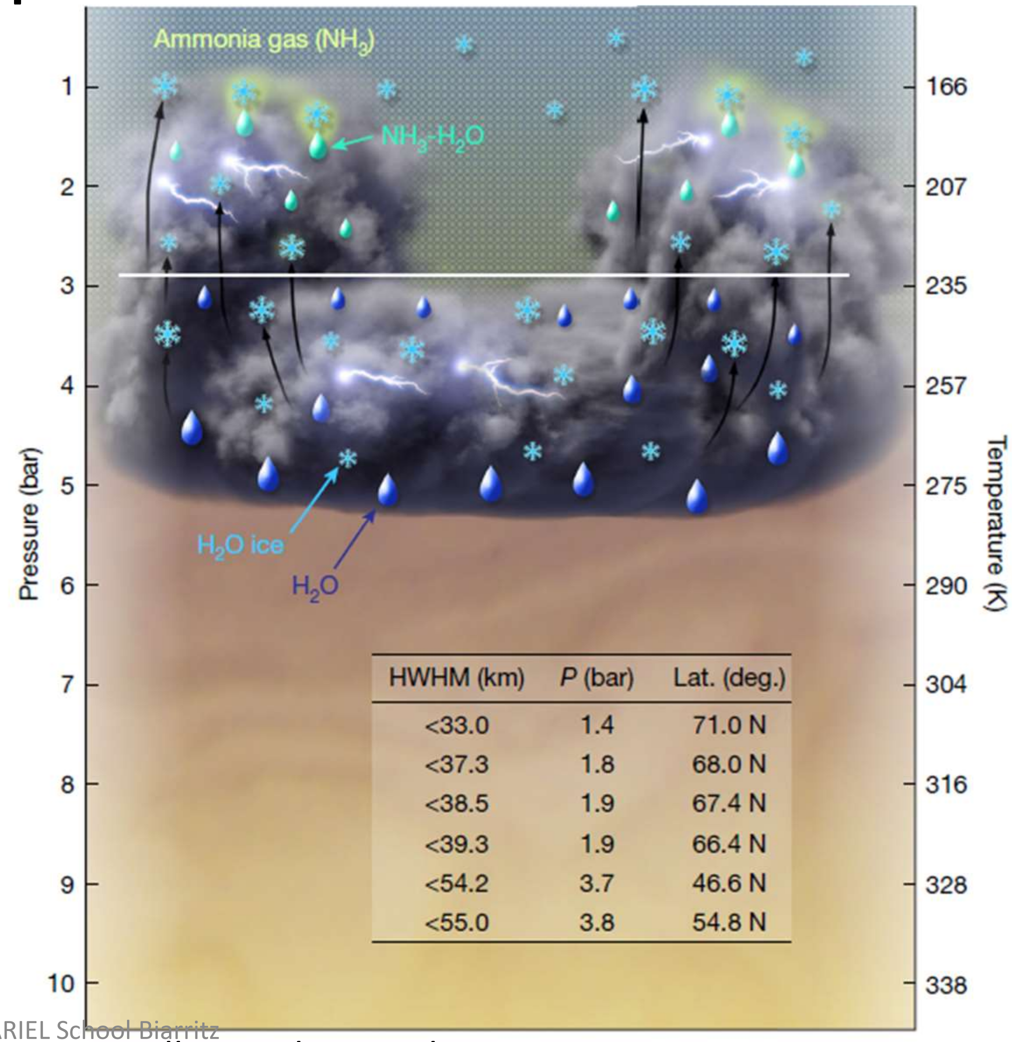

HWHM (km)	*P* (bar)	Lat. (deg.)
<33.0	1.4	71.0 N
<37.3	1.8	68.0 N
<38.5	1.9	67.4 N
<39.3	1.9	66.4 N
<54.2	3.7	46.6 N
<55.0	3.8	54.8 N

Guillot et al., JGR planets, I. Fig. 3

Phase diagrams on Jupiter (H_2O, NH_3)

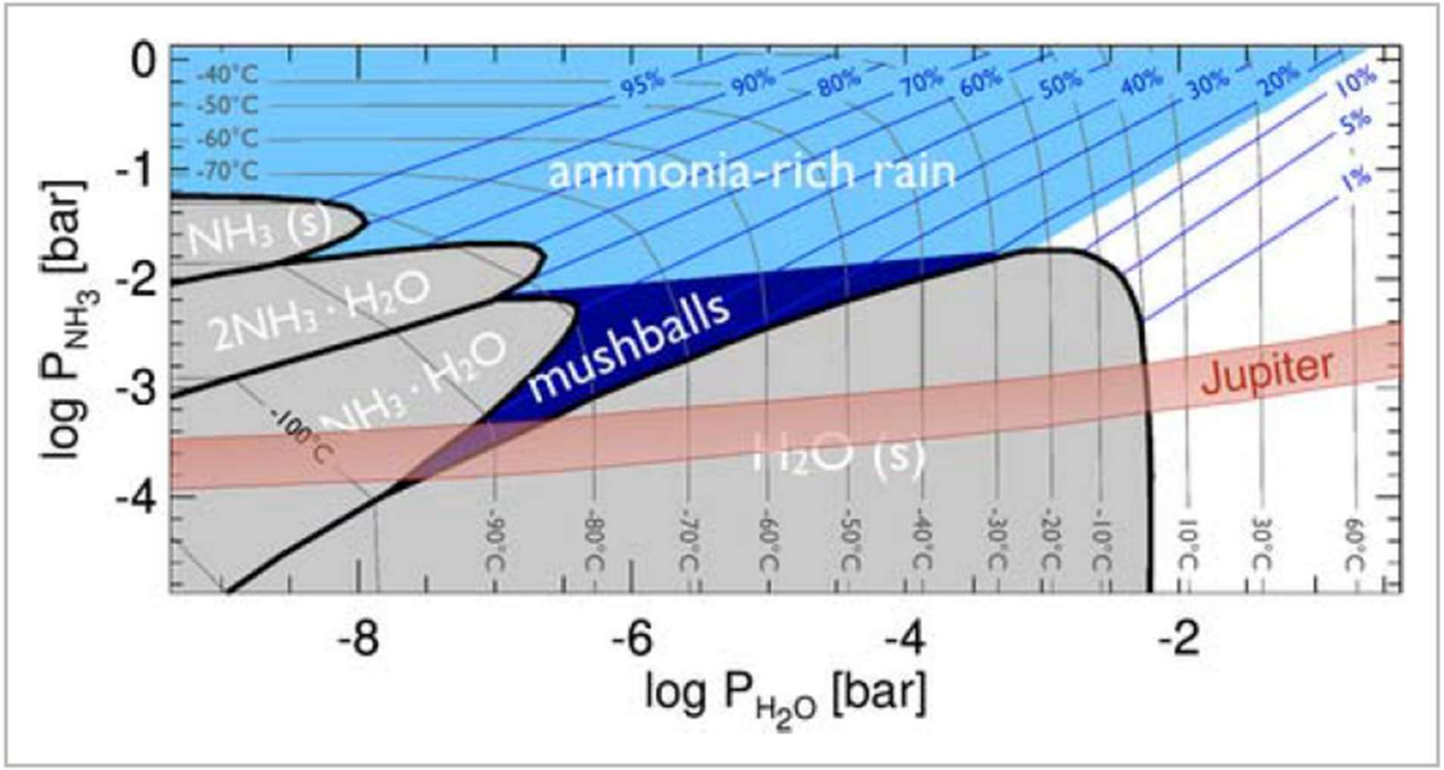

Guillot et al., JGR planets, I. Fig. 1

H_2O-NH_3 equilibrium phase diagram (from Weidenschilling & Lewis, 1973)
Solid phases in gray. Liquid mixture forms in blue

Mixing milk in water

Guillot et al., JGR planets, I. Fig. 5

Figure 5. Simple experiment to illustrate the importance of localized downdrafts in fluid mixtures. Here, at $t = 0$, a tea spoon of fat milk from the refrigerator (~10°C) is added to a glass of water at room temperature (~20°C). Although the milk would be able to dissolve homogeneously in the glass, its slightly higher density resulting from its higher mean molecular weight and lower temperature yields strongly localized downdrafts. The final state is characterized by a gradient of increasing milk concentration with depth. Similarly, we expect strong storms in Jupiter to deliver to about 10 bar a cold and relatively highly concentrated water- and ammonia-rich gas leading to downdrafts able to reach the deeper levels of the planets. Individual storms should have horizontal extents of about ~25 km (Hueso et al., 2002) and Juno measurements indicate that ammonia concentration increases on a vertical scale of at least 100 km. Although this is largely coincidental, we note that the geometry for that simple experiment is relatively similar to that in Jupiter.

Average map of ammonia abundance of Jupiter as observed by Juno/MWR

Average map of NH_3 abundance from Juno/MWR vs latitude & pressure. The model mechanisms (convection/storms/ condensation are superimposed

Water vapor codenses to ice particle at ~ 5 bar level

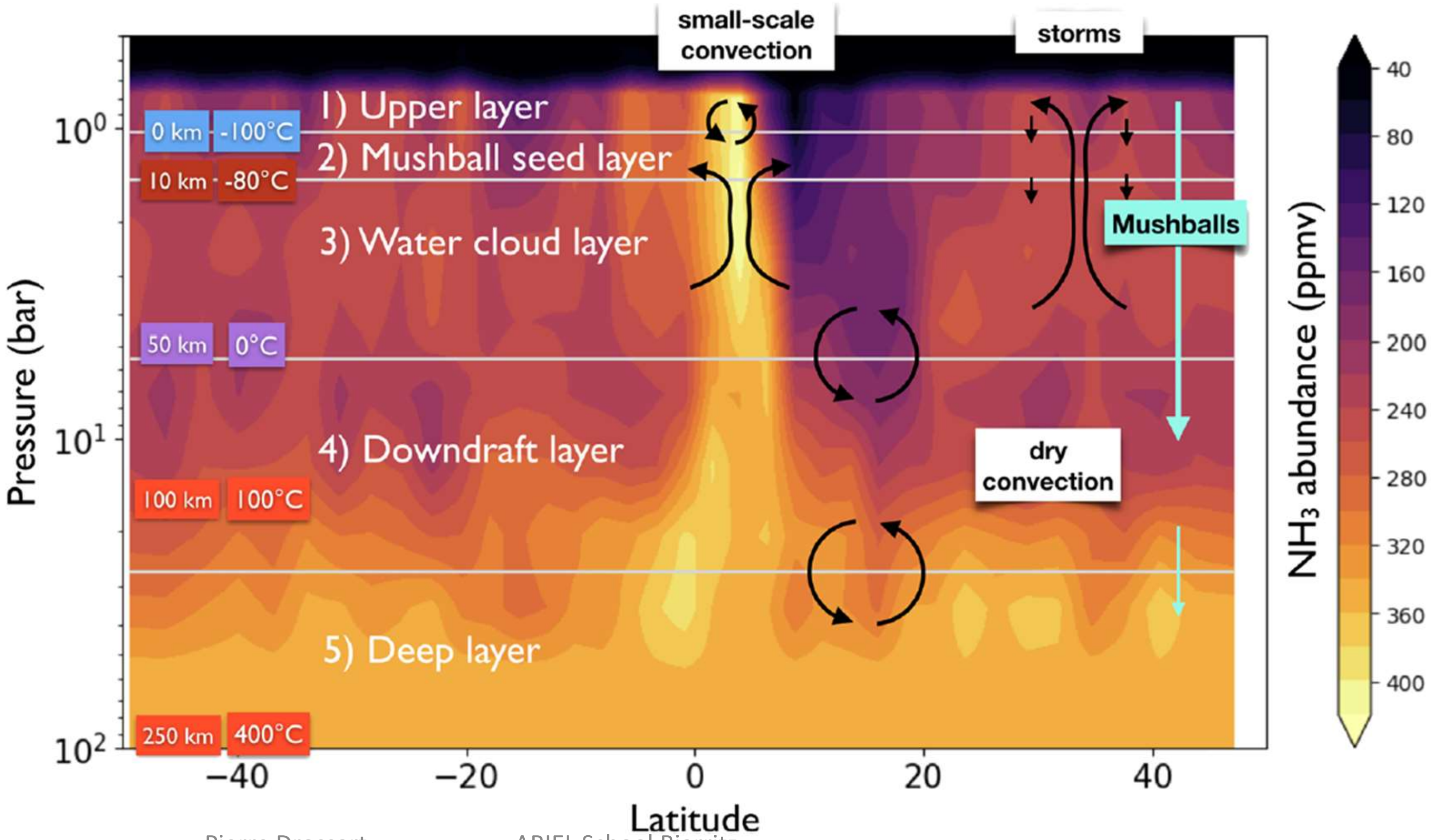

Guillot et al., JGR planets, II. Fig. 1

Anomalies in H_2O, NH_3 and potential temperatures vs convection parameters

- Abundances of water, ammonia and potential-temperature anomalies
- f_{storm} is measure of the mass flux (as compared to dry convection)
- f_{conv} is the small-scale convection factor
- Left : no small-scale convection (midlatitudes)
- Right both scale convection+storms

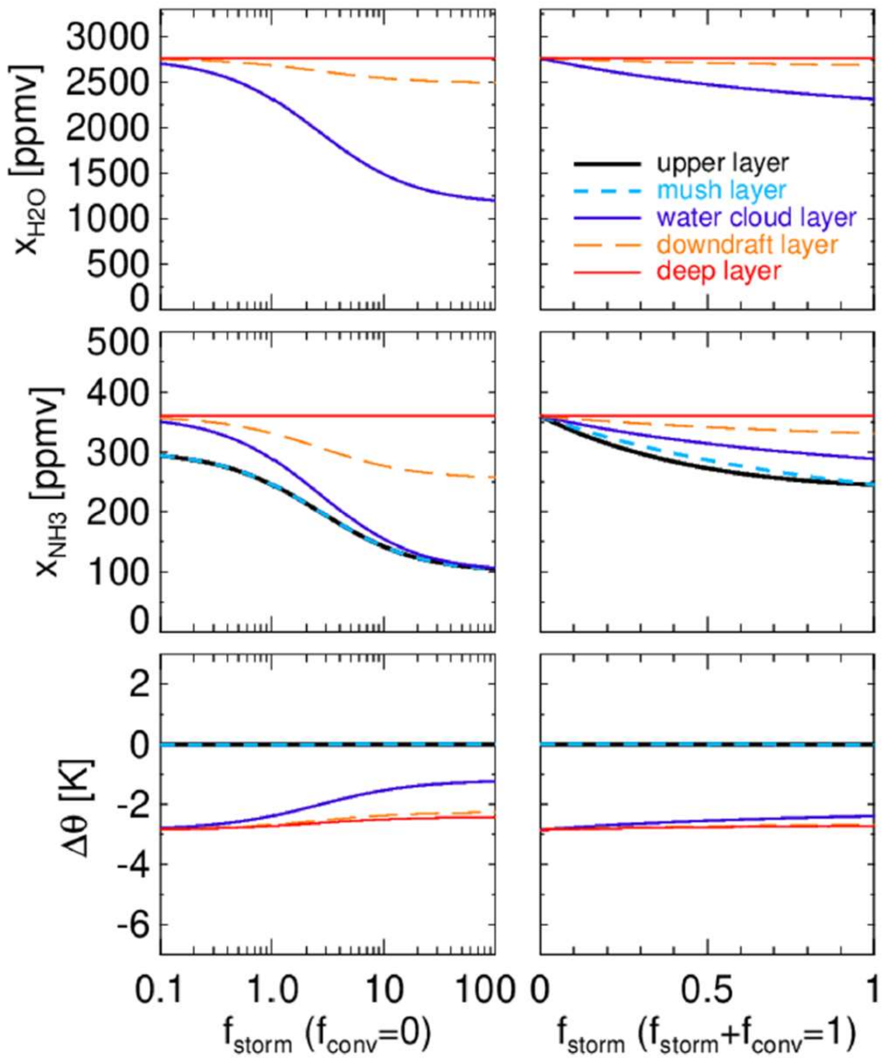

Guillot et al., JGR planets, II. Fig. 5

Ammonia depletion vs latitude : fit of MWR observations

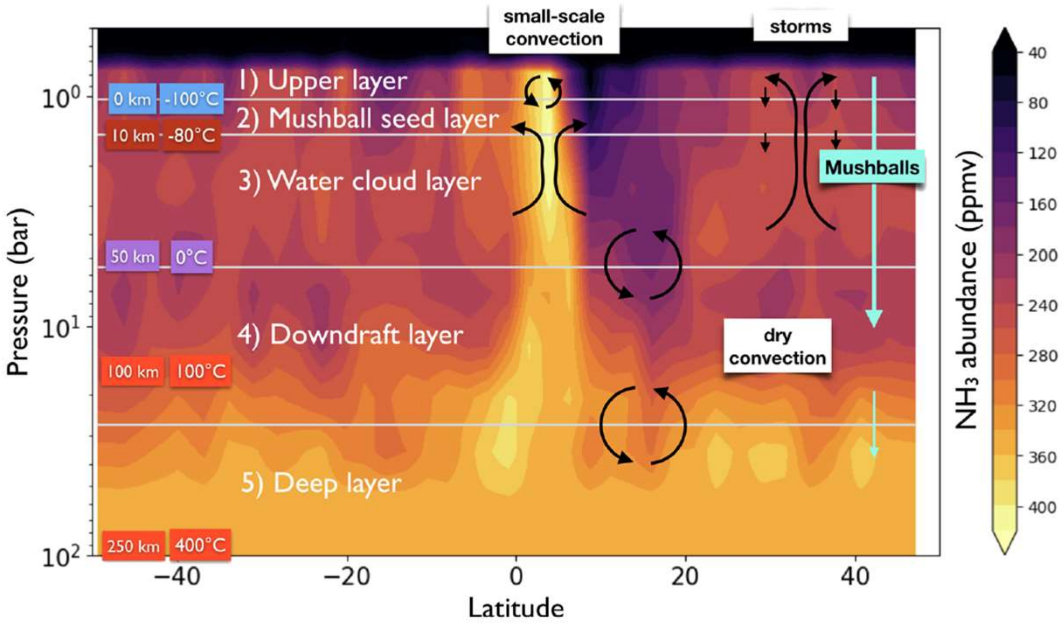

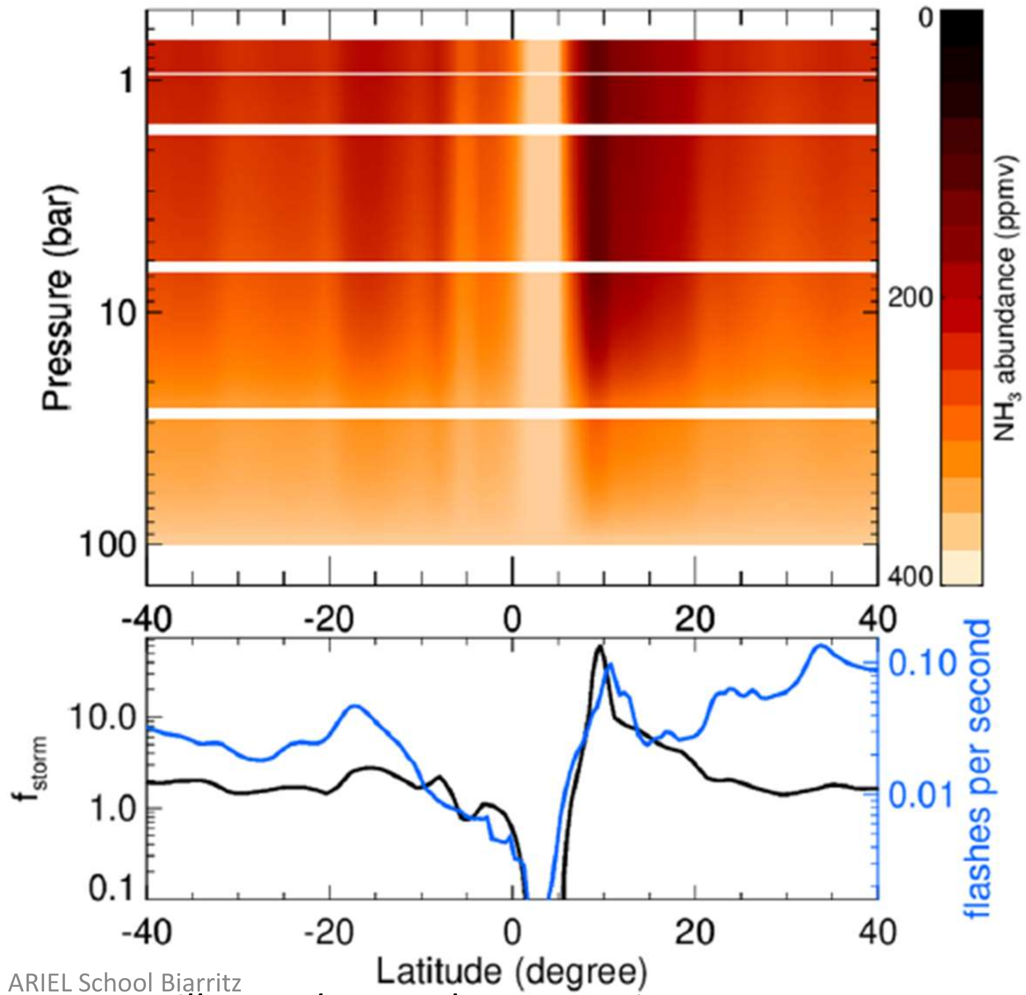

Guillot et al., JGR planets, II. Fig. 6

Conclusions of the studies

Strong Storms, which are located away from the Equatorial Zone in middle latitudes, deliver disequilibrium species from deep levels to elevate their abundance relative to the equator, but they tend to remove ammonia at middle latitudes through the mushball process

Generalization of the process to other planets

Uranus & Neptune depletion in NH_3 ?

« mushball » precipitation must occur much deeper in non-observable layers, but may give the same process on the condensable species with depletion of NH3

What about exoplanets ?

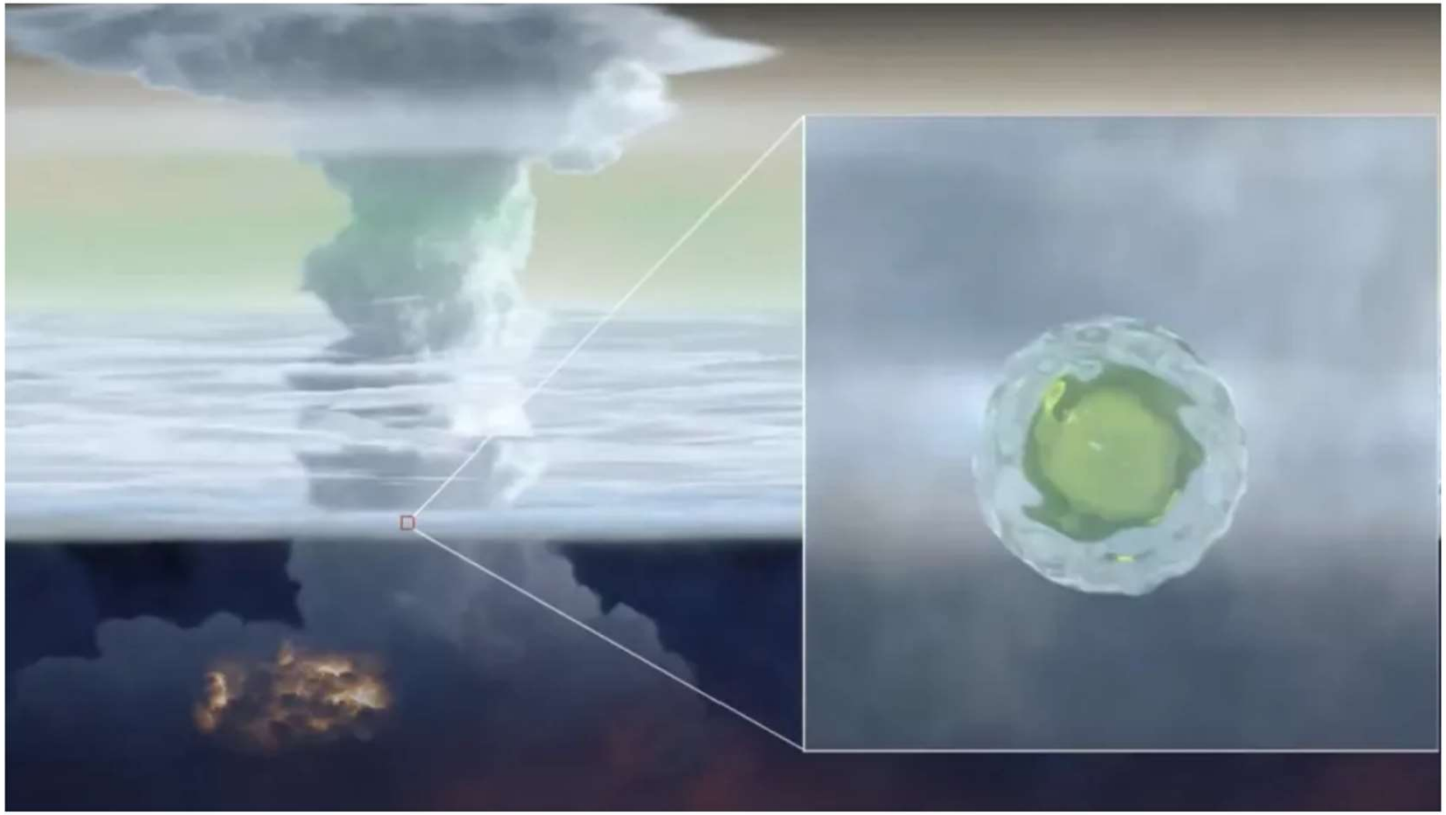

Artist's impression of a mushball descending through a giant planet's atmosphere. (Image credit: NASA/JPL-Caltech/SwRI/CNRS)

Water clouds on K2-18b

Formation and dynamics of water clouds on temperate sub-Neptunes: the example of K2-18b

B. Charnay[1], D. Blain[1], B. Bézard[1], J. Leconte[2], M. Turbet[3], and A. Falco[2]

Context. *Hubble* Space Telescope (HST) spectroscopic transit observations of the temperate sub-Neptune K2-18b were interpreted as the presence of water vapour with potential water clouds. 1D modelling studies also predict the formation of water clouds in K2-18b's atmosphere in some conditions. However, such models cannot predict the cloud cover, which is driven by atmospheric dynamics and thermal contrasts, and thus neither can they predict the real impact of clouds on spectra.
Aims. The main goal of this study is to understand the formation, distribution, and observational consequences of water clouds on K2-18b and other temperate sub-Neptunes.
Methods. We simulated the atmospheric dynamics, water cloud formation, and spectra of K2-18b for a H_2-dominated atmosphere using a 3D general circulation model. We analysed the impact of atmospheric composition (with metallicity from 1× solar to 1000× solar), concentration of cloud condensation nuclei, and planetary rotation rate.
Results. Assuming that K2-18b has a synchronous rotation, we show that the atmospheric circulation in the upper atmosphere essentially corresponds to a symmetric day-to-night circulation with very efficient heat redistribution. This regime preferentially leads to cloud formation at the sub-stellar point or at the terminator. Clouds form at metallicity $\geqslant$100× solar with relatively large particles (radius = 30–450 μm). At 100–300× solar metallicity, the cloud fraction at the terminators is small with a limited impact on transit spectra. At 1000× solar metallicity, very thick clouds form at the terminator, greatly flattening the transit spectrum. The cloud distribution appears very sensitive to the concentration of cloud condensation nuclei and to the planetary rotation rate, although the impact on transit spectra is modest in the near-infrared. Fitting HST transit data with our simulated spectra suggests a metallicity of ~100–300× solar, which is consistent with the mass-metallicity trend of giant planets in the Solar System. In addition, we found that the cloud fraction at the terminator can be highly variable in some conditions, leading to a potential variability in transit spectra that is correlated with spectral windows. This effect could be common on cloudy exoplanets and could be detectable with multiple transit observations. Finally, the complex cloud dynamics revealed in this study highlight the inherent 3D nature of clouds shaped by couplings between microphysics, radiation, and atmospheric circulation.

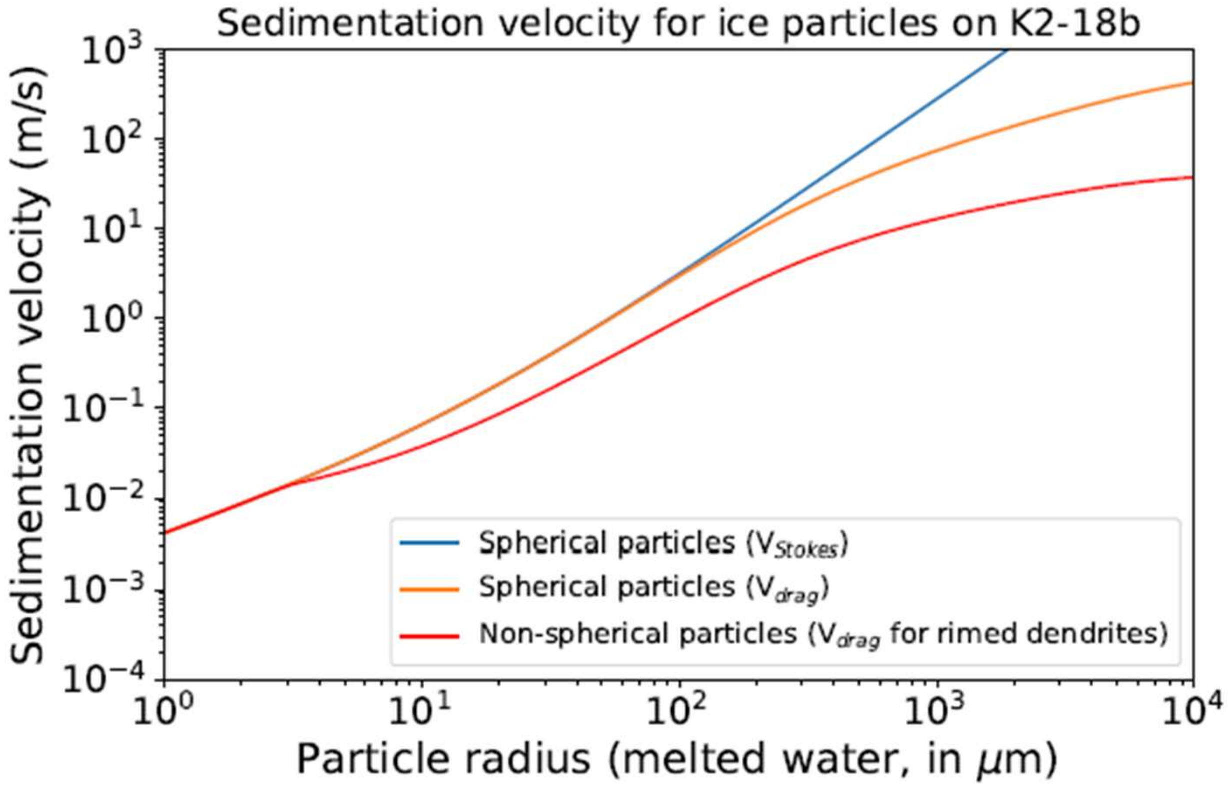

Fig. 1. Sedimentation velocity as a function of particle radius (equivalent radius of melted water) computed for K2-18b at 10^3 Pa. The blue line follows the Stokes law for spherical particles. The yellow line shows the terminal velocity for the general drag coefficient. The red line is computed with the general drag coefficient and for rimed dentrites (parametrisation from Heymsfield 1977).

Physical processes included in a cloud model

Water cloud model :

- Condensation
- Evaporation
- Coalescence
- Sedimentation

Temperature profiles for different metallicities Crossing the condensation curve

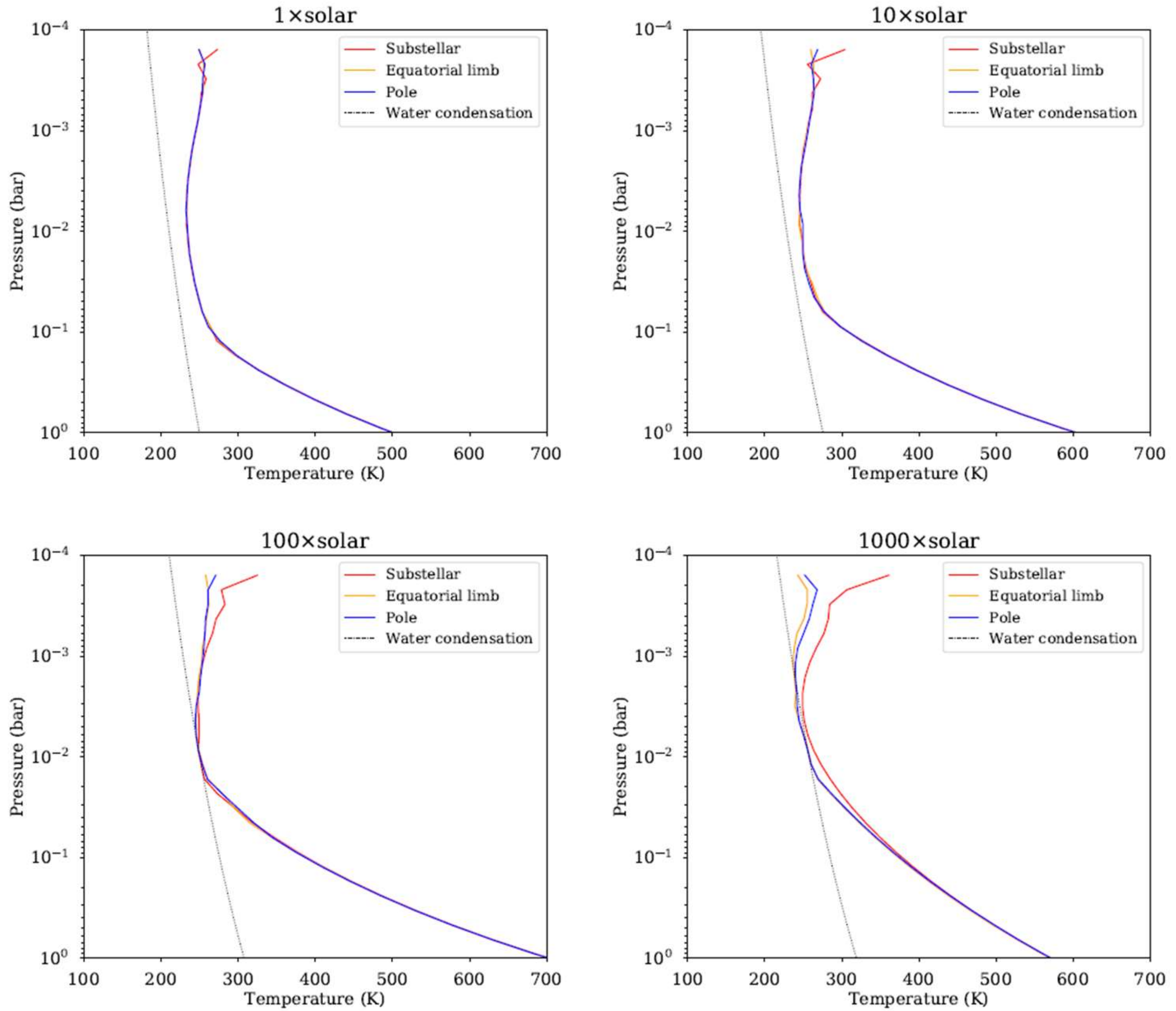

Fig. 2. Temperature profiles for 1×, 10×, 100×, and 1000× solar metallicity at the sub-stellar point (red) at poles (blue) and at the equatorial morning terminator (yellow). The dashed lines are the condensation curves of water vapour.

Radiative cooling and cloud formation for a synchronous rotation planet

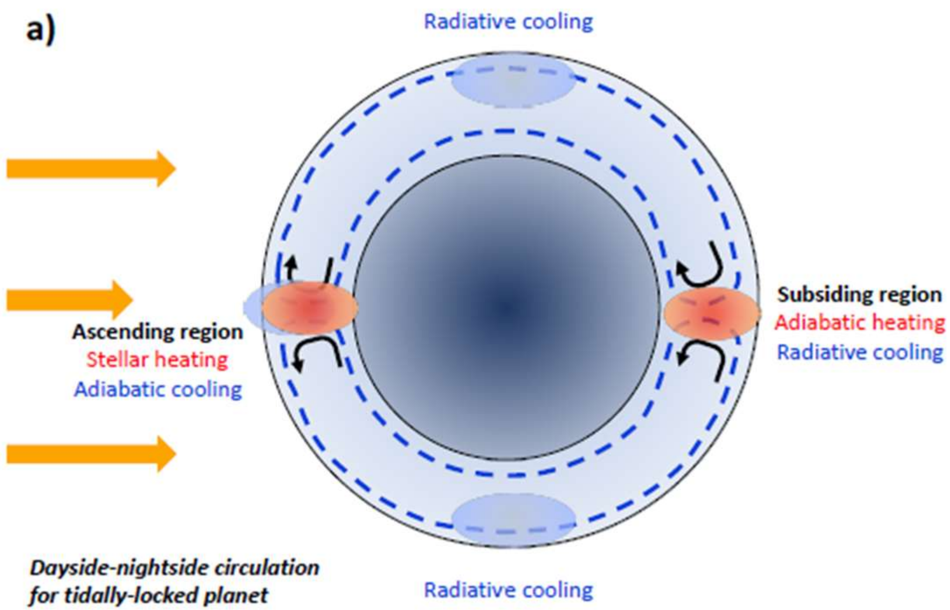

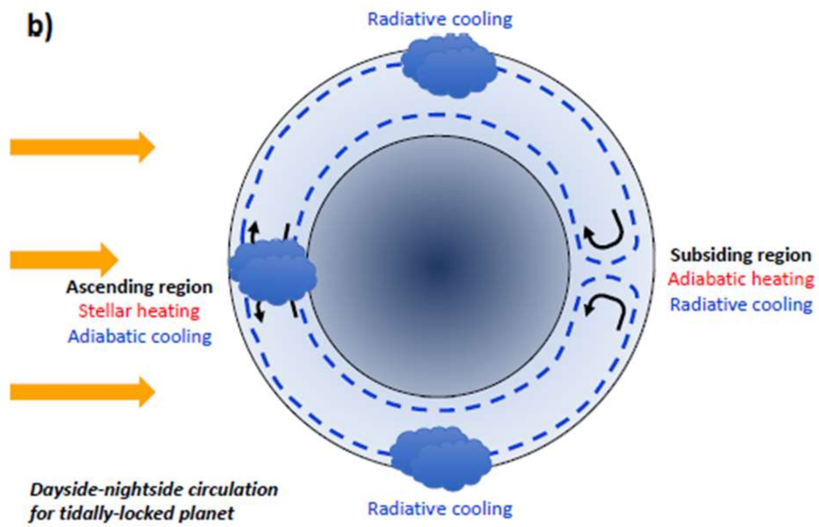

Fig. 4. Illustration of day-night atmospheric circulation around K2-18b for a synchronous rotation. *Panel a*: circulation and warming/cooling zones. *Panel b*: preferential location of cloud formation.

References

- Articles quoted in this presentation

Guillot et al, 2019

Charnay et al, 2021

Hansen & Hovenier, 1974

West et al., 2001

(see complete reference list in separate document)

For more information, see :